Front. Archit. Civ. Eng. China 2011, 5(4): 518–524
DOI 10.1007/s11709-011-0128-4

RESEARCH ARTICLE

Yong QUAN, Yi LIANG, Fei WANG, Ming GU

Wind tunnel test study on the wind pressure coefficient of claddings of high-rise buildings

Abstract The area-averaged most unfavorable wind pressure coefficients (MUWPCs) on various regions of building surfaces and the influence of the side ratio and the terrain category were studied based on wind tunnel test data of scale models of typical high-rise buildings with rectangular cross-sections. The negative area-averaged MUWPCs in the middle-height edge areas generally increased with an increasing D/B side ratio. The area-averaged MUWPCs can be well fitted with a function of the average area reduced by the square of the building depth, D^2. In addition, no unique pattern was found for the effect of the terrain category on the MUWPCs.

Keywords side ratio, area-averaged pressure coefficients, cladding, terrain category

1 Introduction

Because of the large-scale popularization and application of cladding, accidents involving cladding that are caused by strong winds occur frequently, leading to great economic losses and mass casualties. For the purpose of designing cladding economically and safely, the area-averaged most unfavorable wind pressure coefficients (MUWPCs) should be identified accurately. In practical engineering, there is usually a need to conduct a wind tunnel test for high-rise buildings before construction to ensure the distribution rule of the area-averaged MUWPCs on their surface. However, due to the restriction of the test equipment and the consideration of the economic cost, only sparse test taps are arranged on the surface of the test model in actual practice. The MUWPCs accessed by these test taps are taken as the reference frame of the cladding design. However, this design approach causes unnecessary waste because of the size reduction effect.

The initial research investigating the area-averaged wind pressure on cladding began in the 1970s. Marshall [1] conducted field measurements on a single-layer house and a wind tunnel test of its model, obtaining the extreme value of the wind pressure on the roof surface with a weighted average processing to the time history data. The results showed that the extreme value of the wind pressure significantly decreases with the increase of the area. Davenport et al. [2,3] conducted a more systemic study on the wind pressure distribution rule on low-rise buildings, including the influence of the roof pitch, aspect ratio, building height, scaling factor, terrain category and building construction, such as eaves and parapets, on the area-averaged wind pressure on the cladding in the eaves and the rigid corner areas. In addition, a preliminary study of the size reduction rule was also conducted.

Since the 1980s, the multichannel pressure measurement system has been widely used for low-rise buildings, long-span roofs, and high-rise buildings [4–6]. A large number of taps in the wind tunnel test models can be arranged, and the study regions are not limited to the flow separation zone, such as the roof corner. Furthermore, the means of measuring the area-averaged wind pressure also include embedded film sensors [7], through-hole polyethylene [8], piezoelectric polymer films [9], and so on. These research results are helpful for understanding the space-time distribution of the wind pressure on the surface of a structure and contribute to the further research on the size reduction rule for the wind pressure on the cladding.

After 1995, with the development of test techniques and equipment, simultaneous multipressure measurements of a large number of test taps have been realized, from which a more detailed study of their distribution rules has been achieved. However, the study contents have not changed

Received September 11, 2011; accepted October 8, 2011

Yong QUAN (✉), Fei WANG, Ming GU
State Key Laboratory for Disaster Deduction in Civil Engineering, Tongji University, Shanghai 200092, China
E-mail: quanyong@tongji.edu.cn

Yi LIANG
Shanghai Nuclear Engineering Research and Design Institute, Shanghai 200233, China

greatly because these mainly included the size reduction rule in the flow separation zone of the low-rise buildings and the relevant analysis of the wind pressure on the surface of buildings and so on [10–12].

Overall, most of the previous studies focused on wind loads on the cladding of low-rise buildings, and their findings have been applied in codes and standards. However, such studies are still insufficient.

In the present study, a method of calculating the area-averaged MUWPCs for cladding on high-rise buildings is introduced. Furthermore, the area-averaged MUWPCs on various regions of typical high-rise buildings with rectangular cross-sections as well as the influence of aspect ratio and terrain category are studied based on wind tunnel test data.

2 Wind tunnel test

The wind-tunnel test was conducted in simulated wind fields of types A, B, C, and D [13] in a wind tunnel in Tongji University, Shanghai, China. The simulated results of wind field B are shown in Fig. 1. According to the data and the fitting formula provided by the Architectural Institute of Japan (AIJ) [14], the turbulence length scale was specially simulated (Fig. 1(b)). The scale ratios of length, wind velocity, and time in this test were 1/250, 1/5 and 1/50, respectively. The sampling frequency and sampling time of the wind pressure were 312.5 Hz and 48 s, corresponding to 6.25 Hz and 240 s in full scale, respectively. The heights of the rigid models were all 90 cm, corresponding to 225 m at full size, a value that is representative of high-rise buildings. Three model cases, namely, M1, M2 and M3, with side ratios of 1.0, 2.0 and 0.5, respectively, were tested. There were serried measuring taps on the surfaces of the different areas of the models, representing the upper edge (*A*1), central edge (*A*2 and *A*3), lower edge (*A*4), and central inner (*A*5 and *A*6) regions (Fig. 2).

3 Test data processing

The time series of the wind pressures, $p(\theta,i,t)$, at tap i on a model surface measured in the test for a wind direction angle of θ was divided by the tested approaching wind pressure, $0.5\rho_a V_H^2$, at the height of the model, from which the time series of the wind pressure coefficient, $C_p(\theta,i,t)$, was obtained. The area-averaged pressure coefficient, $C_{pA}(\theta,t)$, was calculated by means of $C_p(\theta,i,t)$ on all measuring taps within a target area, A, which was weight-averaged by subsidiary area, A_i, i.e.,

$$C_{pA}(\theta,t)=\sum_{i=1}^{n}A_iC_p(\theta,i,t)/\sum_{i=1}^{n}A_i.$$

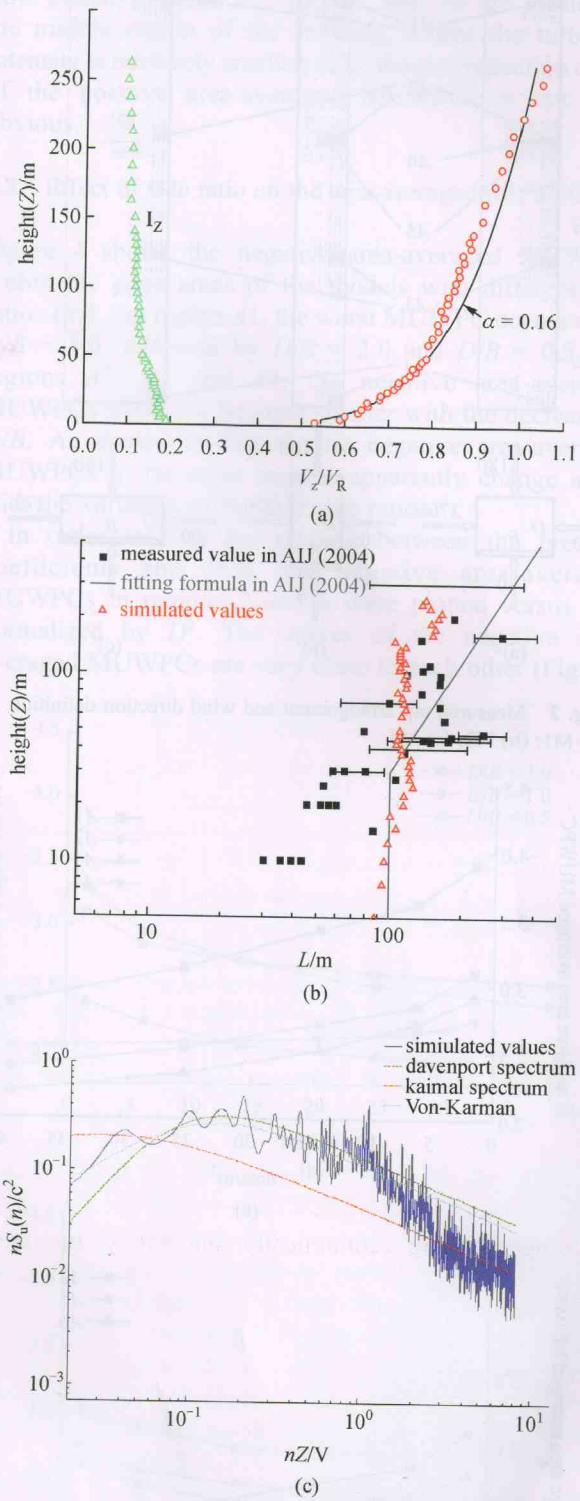

Fig. 1 Mean velocity, turbulence intensity profile, and velocity spectrum for simulated wind field B. (a) Mean velocity profile; (b) turbulence intensity profile; (c) velocity spectrum (at the height of 112.5 m)

The extreme values, $\hat{C}_{pA}(\theta)$ or $\check{C}_{pA}(\theta)$, of $C_{pA}(\theta,t)$ were calculated using the Sadek-Simiu method [15]. By

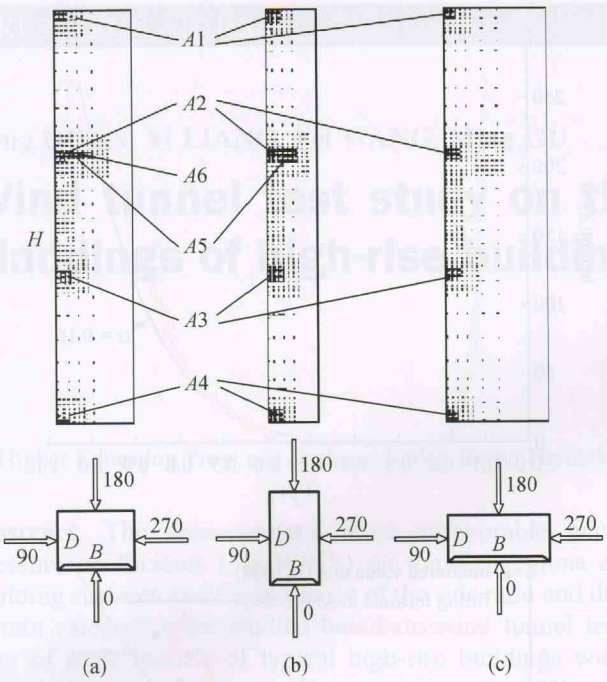

Fig. 2 Measured tap arrangement and wind direction definition. (a) M1; (b) M2; (c) M3

choosing the maximum value of $\hat{C}_{pA}(\theta)$ and the minimum value of $\check{C}_{pA}(\theta)$ for any wind direction angle, θ, the positive and negative area-averaged MUWPCs, $C^{\wedge}_{pA\_\max}$ and $C^{\vee}_{pA\_\min}$, respectively, were obtained.

4 Test results

4.1 Effect of location on the area-averaged MUWPCs

It can be observed from Fig. 3 that the negative area-averaged MUWPCs are very large in region $A1$, where the coefficients are generally beyond -3.9. In regions $A2$ and $A3$, which are less affected by the three-dimensional (3D) effect, the area-averaged MUWPCs under all test cases are similar. Edge region $A4$ is located in the bottom building where high suctions occur. Negative area-averaged MUWPCs in this area are very large in some test cases but are still very close to those in middle edge regions $A2$ and $A3$ in most cases. In addition, the size reduction effect of the negative area-averaged MUWPCs of region $A1$ is the largest, followed by regions $A2$ and $A3$, with region $A4$

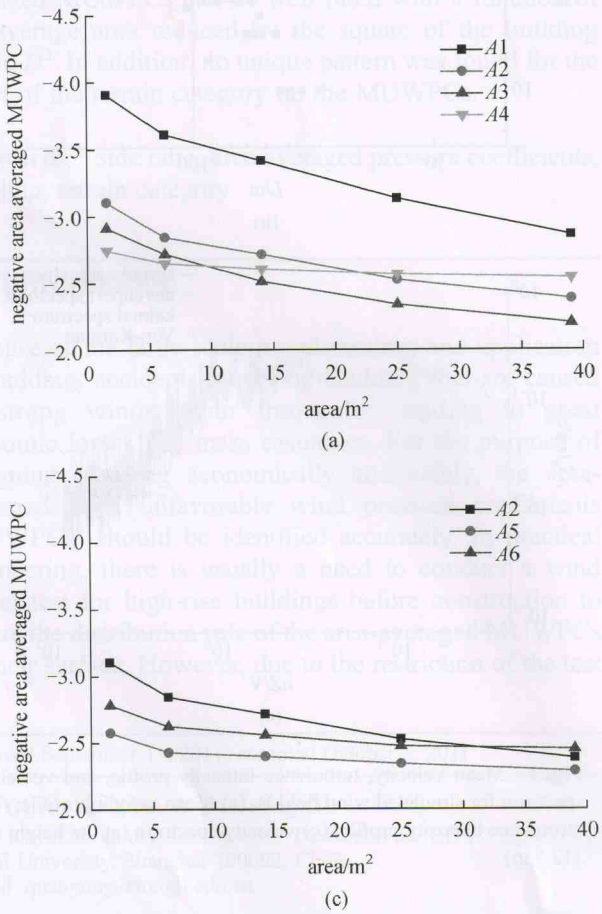

Fig. 3 Effect of location on the most unfavorable negative area-averaged wind pressure coefficients. (a) Edge area of M1 in wind field type B; (b) edge area of M2 in wind field type D; (c) inner area of M1 in wind field type B; (d) inner area of M2 in wind field type D

being the smallest. Apart from different distribution patterns in regions of different height, the pressure distributions in the wall edges and inner regions of a high-rise building are also different. From Fig. 3(c), for the area-averaged MUWPCs corresponding to a small area, the values within the edge area are greater than those within the inner area. However, negative area-averaged MUWPCs within the edge area are significantly reduced as the area increases; in some cases, most area-averaged MUWPCs in the edge area are even smaller than those in the inner area.

In general, the positive area-averaged MUWPCs become larger with the increase of the height of the area. However, area 1 is an exceptional case due to 3D turbulence. The positive area-averaged MUWPCs in this area may be larger or smaller than those in regions 2 and 3. The size reduction effect of the positive area-averaged MUWPCs is closely related to turbulence intensity. Region *A*4 is located at the bottom, where the turbulence intensity is comparatively large; thus, the size reduction effect is significant. Region *A*1 is located at the top of the building; thus, the size reduction is also significant because of the 3D flow effect. Regions *A*2, *A*3, *A*5, and *A*6 are located in the middle region of the building, where the turbulent intensity is relatively smaller; thus, the size reduction effect of the positive area-averaged MUWPCs is not very obvious.

4.2 Effect of side ratio on the area-averaged MUWPCs

Figure 4 shows the negative area-averaged MUWPCs within the edge areas of the models with different side ratios *D*/*B*. For region *A*1, the worst MUWPC occurs when *D*/*B* = 1.0, followed by *D*/*B* = 2.0 and *D*/*B* = 0.5. For regions *A*2, *A*3 and *A*4, the negative area-averaged MUWPCs generally become smaller with the decrease of *D*/*B*. As shown in Fig. 4, the negative area-averaged MUWPCs in the edge regions apparently change along with the variation of the *D*/*B* side ratios.

In order to find the relation between the pressure coefficients and *D*/*B*, the negative area-averaged MUWPCs in regions 2 and 3 were plotted versus area normalized by D^2. The curves of the negative area-averaged MUWPCs are very close to each other (Fig. 5).

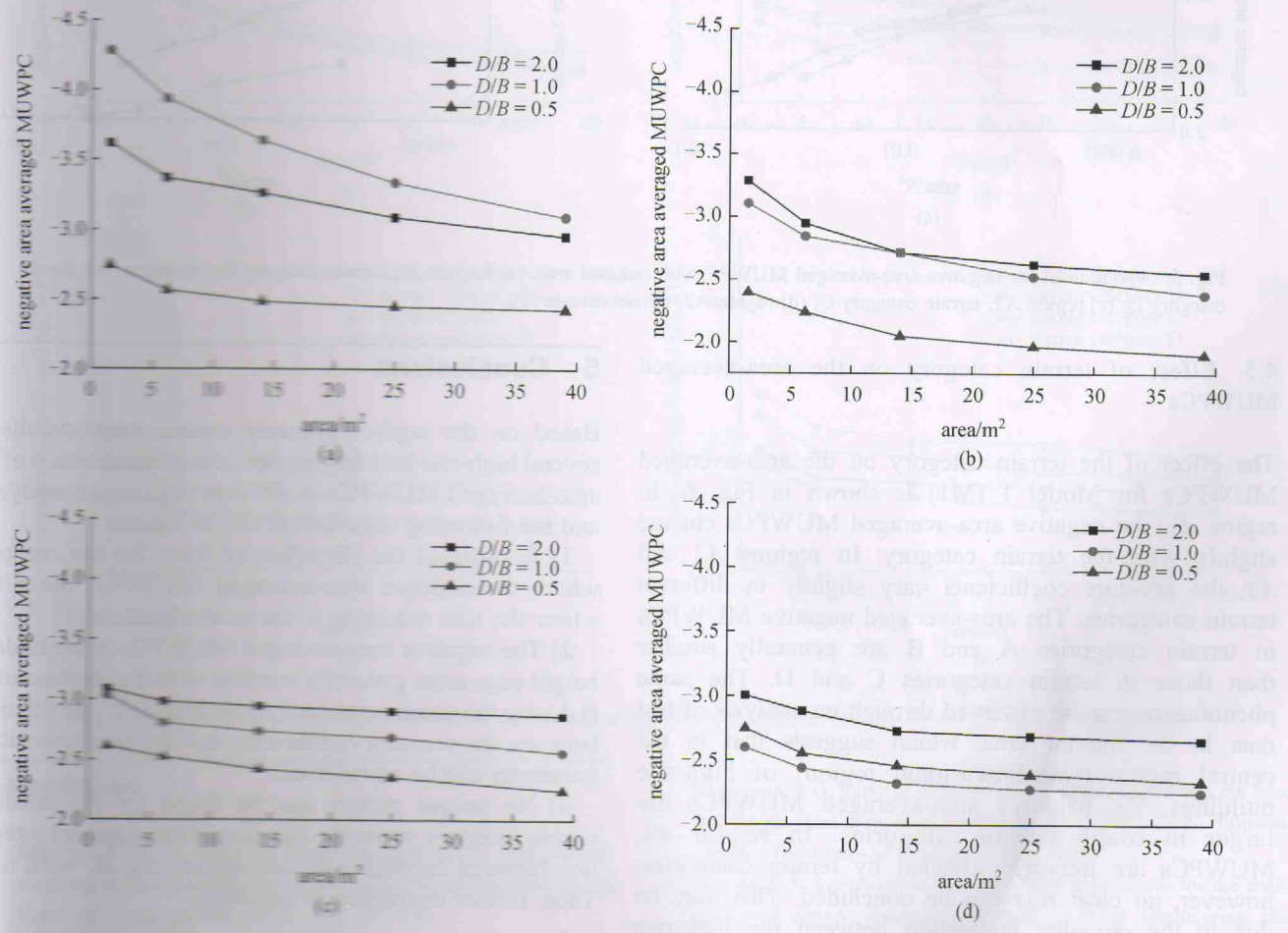

Fig. 4 Effect of aspect ratio *D*/*B* on the negative area-averaged MUWPCs. (a) Region *A*1, wind field type A; (b) region *A*2, wind field type B; (c) region *A*3, wind field type C; (d) region *A*4, wind field type D

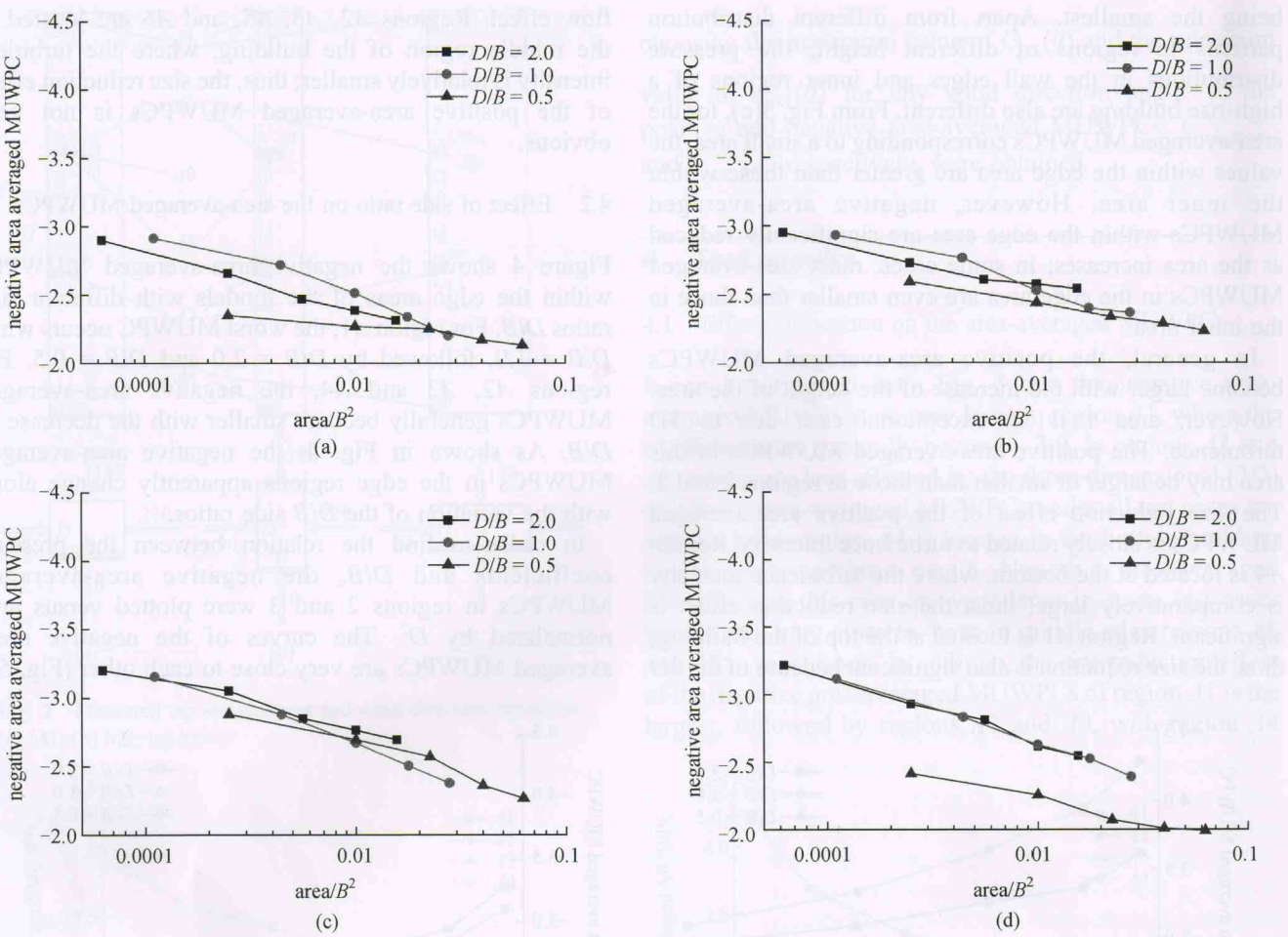

Fig. 5 Variation of the negative area-averaged MUWPC with reduced area. (a) Region *A*3, terrain category B; (b) region A3, terrain category D; (c) region A2, terrain category C; (d) region A2, terrain category A

4.3 Effect of terrain category on the area-averaged MUWPCs

The effect of the terrain category on the area-averaged MUWPCs for Model 1 (M1) is shown in Fig. 6. In region *A*1, the negative area-averaged MUWPCs change slightly with the terrain category. In regions *A*2 and *A*3, the pressure coefficients vary slightly in different terrain categories. The area-averaged negative MUWPCs in terrain categories A and B are generally smaller than those in terrain categories C and D. The same phenomenon can be observed through an analysis of test data in the interior area, which suggests that in the central region (two-dimensional region) of high-rise buildings, the negative area-averaged MUWPCs are larger in rough terrain categories. In region *A*4, MUWPCs are intensely affected by terrain categories; however, no clear rule can be concluded. This may be due to the complex interaction between the high-rise building and the 3D wind field, thus requiring further discussion.

5 Conclusions

Based on the surface pressure measurement results of several high-rise building models, the characteristics of the area-averaged MUWPCs in different regions are analyzed, and the following conclusions can be drawn:

1) Because of the 3D effect of flow, the top corner is where the negative area-averaged MUWPCs occur and where the size reduction is the most significant.

2) The negative area-averaged MUWPCs in the middle-height edge areas generally increase with the increase of D/B. Using the nondimensional parameter, A/D^2, the relations between the pressure coefficients and the nondimensional parameter can be represented.

3) No unique pattern can be found for the effect of terrain category, probably because of the complex interaction between the high-rise building and the 3D wind field. Thus, further discussion is required.

Acknowledgements This research was supported by the National Natural Science Foundation of China (Grant Nos. 50878159 and 90715040).

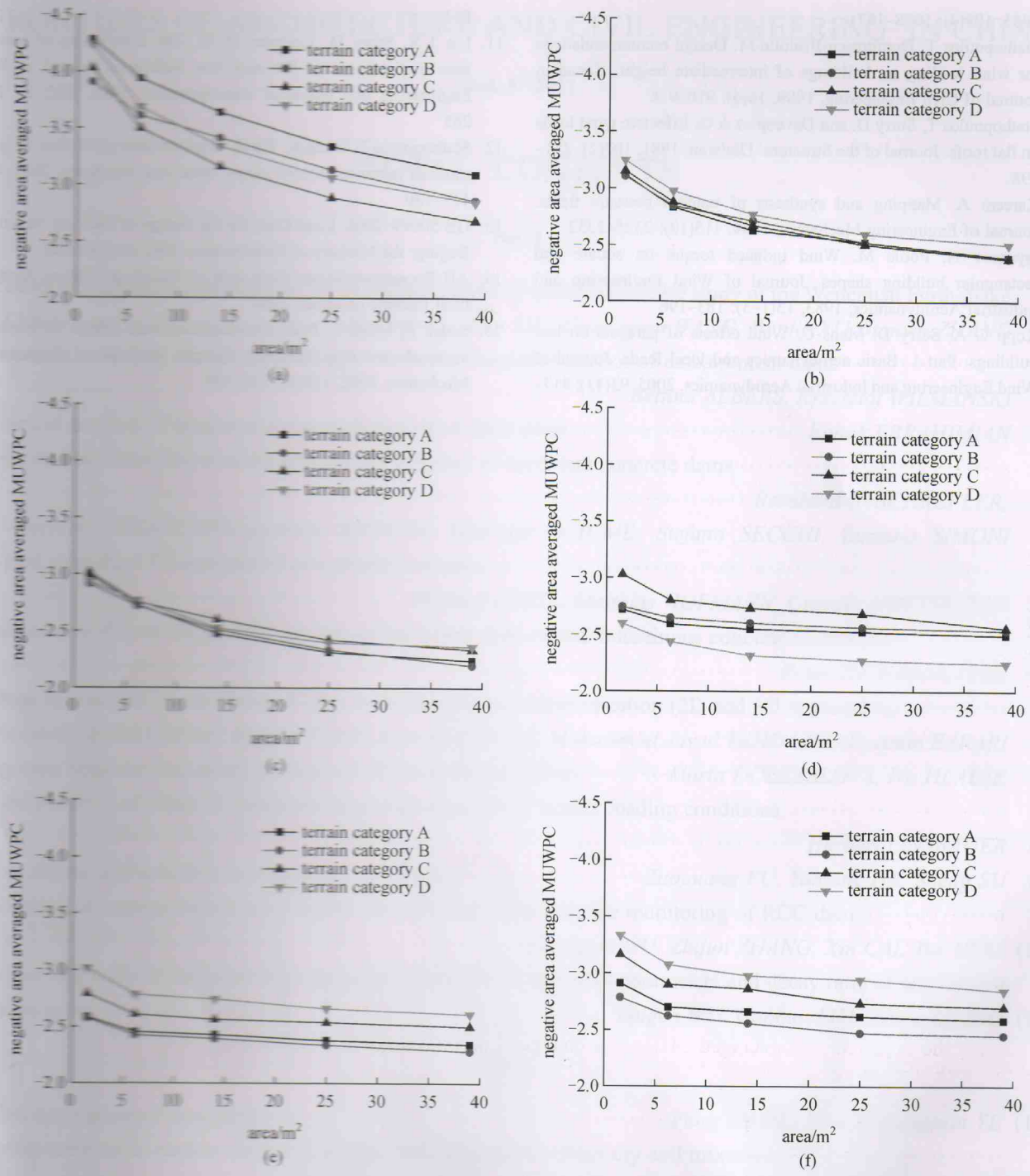

Fig. 6 Effects of the terrain categories on the area-averaged MUWPCs for M1. (a) *A*1; (b) *A*2; (c) *A*3; (d) *A*4; (e) *A*5; (f) *A*6

References

1. Marshall R D. A study of wind pressures on a single-family dwelling in model and full scale. Journal of Wind Engineering and Industrial Aerodynamics, 1975, 1(2): 177–199
2. Davenport A G, Surry D, Stathopoulos T. Wind Loads on Low Rise Buildings: Final Report of Phases I and II BLWT-SS8–1977. London, Ontario: University of Western Ontario, 1977
3. Davenport A G, Surry D, Stathopoulos T. Wind Loads on Low Rise Buildings: Final Report of Phases III BLWT-SS8–1977. London, Ontario: University of Western Ontario, 1977
4. Gumley S J. A parametric study of extreme pressures for the static design of canopy structures. Journal of Wind Engineering and Industrial Aerodynamics, 1984, 16(1): 43–56
5. Surry D, Stathopoulos T, Davenport A G. Simple measurement techniques for area wind loads. Journal of Engineering Mechanics,

1983, 109(4): 1058–1071

6. Stathopoulos T, Dumitrescu-Brulotte M. Design recommendations for wind loading on buildings of intermediate height. Canadian Journal of Civil Engineering, 1989, 16(6): 910–916
7. Stathopoulos T, Surry D. and Davenport A G. Effective wind loads on flat roofs. Journal of the Structural Division, 1981, 107(2): 281–298
8. Kareem A. Mapping and synthesis of random pressure fields. Journal of Engineering Mechanics, 1989, 115(10): 2325–2332
9. Isyumov N, Poole M. Wind induced torque on square and rectangular building shapes. Journal of Wind Engineering and Industrial Aerodynamics, 1983, 13(1–3): 183–196
10. Kopp G A, Surry D, Mans C. Wind effects of parapets on low buildings: Part 1. Basic aerodynamics and local loads. Journal of Wind Engineering and Industrial Aerodynamics, 2005, 93(11): 817–841
11. Lin J X, Surry D, Tieleman H W. The distribution of pressure near roof corners of flat roof low buildings. Journal of Wind Engineering and Industrial Aerodynamics, 1995, 56(2–3): 235–265
12. Stathopoulos T, Wang K, Wu H. Wind pressure provisions for gable roofs of intermediate roof slope. Wind and Structures, 2001, 4(2): 119–130
13. GB 50009–2001. Load Code for the Design of Building Structures. Beijing: the Ministry of Construction. 2002 (in Chinese)
14. AIJ Recommendations for Loads on Buildings. Tokyo: Architectural Institute of Japan, 2004
15. Sadek F, Simiu E. Peak non-Gaussian wind effects for database-assisted low-rise building design. Journal of Engineering Mechanics, 2002, 128(5): 530–539